PRELIMINARY DESIGN OF A FUEL-CELL-BASED HYBRID-ELECTRICAL UAV

Dries Verstraete*, Luigi Cazzato, Giulio Romeo****
***School of Aerospace, Mechanical and Mechatronic Engineering**
The University of Sydney, Aeronautical Eng Bldg J11, NSW 2006 Australia,
****Department of Mechanical and Aerospace Engineering**
Politecnico di Torino, Corso Duca degli Abruzzi 24, 10129 Torino Italia
Dries.Verstraete@sydney.edu.au; Luigi.Cazzato@studenti.polito.it; giulio.romeo@polito.it

Keywords: *unmanned aircraft, hybrid-electrical propulsion, fuel cell, preliminary design*

Abstract

This paper presents the preliminary design of an unmanned aerial vehicle (UAV) with a hybrid-electrical propulsion system centered around a fuel cell. The propulsion system of the UAV is based on the Aeropak system from Horizon Energy Systems. The paper describes the preliminary design tool that was developed to investigate development challenges of fuel-cell-based UAVs. Trade-off studies for two different fuel tanks sizes are given. The results show that the power available from the fuel cell drives the design towards very high aspect ratio wings. The main restriction on the wing design is the region of laminar separation bubbles, which limits the maximum endurance of the UAV. With a 1.1-litre tank a loiter endurance of around 4.5 hours can be obtained in a typical over-the-hill mission remote-sensing. When a 9-litre tank is used, the endurance increases to over 25 hours. The paper also discusses installation of the fuel-cell power plant in an existing small UAV that will be used as a demonstrator.

1 Introduction

Long endurance small man-portable unmanned aerial vehicles (UAVs) have a significant value as low-cost autonomous reconnaissance, telecommunications and remote-sensing platforms for research, commercial and military missions. Small-scale, electrically powered UAVs are in use for a variety of those missions. For these aircraft electrical propulsion is generally preferred over small reciprocating engines or gas turbines because of the latter's low efficiencies at small sizes [1]. The energy density of existing batteries however limits the mission duration to 1 to 2 hours [2-4].

Fuel cells could be a significant driving force in achieving a longer endurance because of their potential to construct power-plants of high specific energy, their low noise, their rapid refueling capability and improved environmental compatibility [5–7]. These advanced power-plant designs however present implementation challenges that will require new development methods and tools. Fuel cells for instance generally have low specific power (W/kg), whereas high specific power is required to improve aircraft (speed) performance and maneuverability. Aircraft concepts powered solely by fuel cells therefore require both extremely lightweight airframes and low power payloads, and still result in operationally highly constrained designs [7-9]. A hybrid-electrical propulsion chain where secondary power sources with high specific power are added to provide a brief high-power boost capability could alleviate those restrictions leading to a platform with a better overall performance [10-12].

Despite the potential of fuel-cell powered UAVs, little practical knowledge exists about the implementation challenges and compromises associated with making an integrated fuel-cell/aircraft system. The majority of existing studies on fuel-cell aircraft are "high-level" conceptual design studies where the "low-level" compromises between the

aircraft requirements and the characteristics of the power-plant are not addressed explicitly [7, 12]. As details on the few projects that have proven the viability of small-scale fuel-cell-powered UAVs are not publicly available, the design and development challenges of fuel cell UAVs are not well-understood by the general UAV community [7].

To increase this understanding and to develop tools and technologies for design and implementation of fuel cells as power-plants in aircraft, a fuel-cell based hybrid-electrical UAV demonstration program was started by the Micro Propulsion Group of the School of Aerospace, Mechanical and Mechatronic Engineering of The University of Sydney. The primary objectives of the program are: the development of validated tools for the design of fuel-cell based hybrid-electrical propulsion UAVs; the analysis of design trade-offs and optimal configurations of fuel-cell powered UAVs; and to design, build and fly a demonstrator UAV.

The current paper reports the preliminary design and optimization work undertaken as part of this initiative. The first section of the article describes the developed preliminary design model for fuel-cell powered UAVs. Two baseline configurations are determined next and tradeoff studies on key airframe parameters are reported. Finally, installation of the fuel-cell hybrid system in an existing small UAV is described.

2 Preliminary Design Tool

A preliminary design tool was developed to allow the initial exploration of the design space. Figure 1 shows the structure of the developed tool. As shown, input is required for the design mission, the payload and the powerplant. The input consists of the payload dimensions, weight and power consumption, and the propulsion system dimensions, weight and fuel consumption as function of power output. The mission profile has to be input too as detailed in section 3.1. As the design tool is currently set up to allow trade-offs between two different airframe parameters, the selected parameters and their range have to be detailed as well. Based on this input, a number of discipline specific modules are iterated on until convergence is reached. Some of those iterations are depicted in Fig. 1. Several of the modules contain additional internal iterations. The main calculation methods are described below. First the propulsion system is described. After that, the aerodynamic methods are detailed, and some of the component weight functions are given. Finally the stability and performance calculations set up in the tool are commented on.

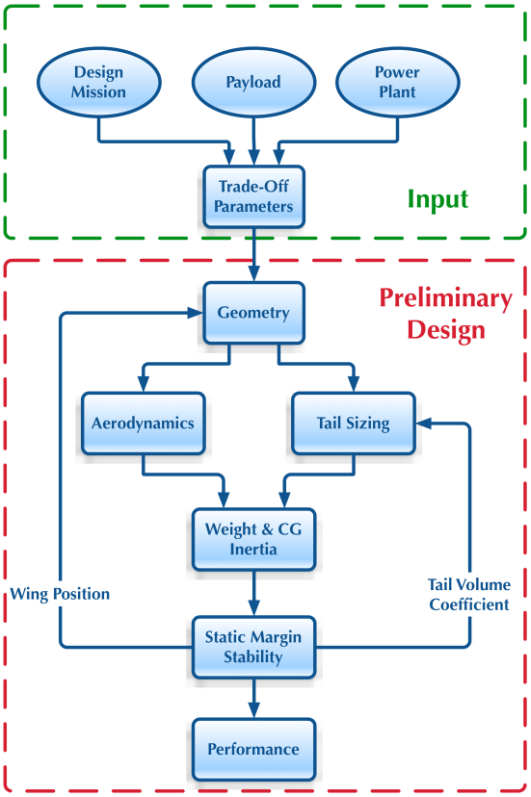

Fig. 1. Structure of the Preliminary Design Tool.

2.1 Propulsion system

The propulsion system is built around the hybrid-electrical fuel-cell based Aeropak system from Horizon Energy Systems [13]. As shown in Fig. 2, the system consists of a 35-cell PEM fuel cell and a 6-cell 1350 mA-hr Li-Po battery pack. The fuel cell can deliver up to 10 A of current and has a nominal power output of 200 W. Its operating voltage ranges from 32 V (no load) to 21 V (full load). The fuel cell is self-humidified and air-cooled and only requires near-ambient cathode pressure. The hydrogen side (anode) is dead-ended, meaning all the hydrogen entering the anode compartment is

either consumed by the fuel-cell reaction or wasted due to leakage.

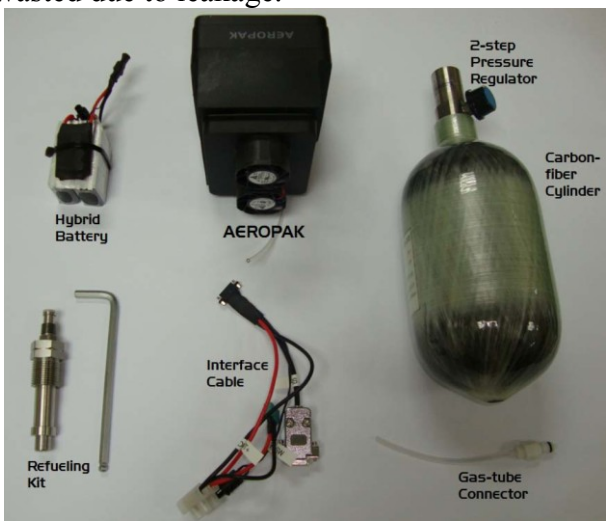

Fig. 2. Components of the hybrid Aeropak fuel-cell/Li-Po battery system from Horizon Energy Systems.

The Li-Po battery is added to the system to provide a power boost capability of an additional 400 W during 2 min to meet the high-power requirements during UAVs take-off or climbing [13]. The power-management board combines the total power output from the fuel cell and battery before delivering it to the load and is limited to 800 W for ~1 min to prevent its diode from overheating [13]. The board additionally recharges the battery when excess power is available from the fuel cell and provides power to the load during the short-circuiting of the fuel cell. The short-circuiting is built into the fuel-cell controller to increase the stack efficiency and forms part of the self-humidification process of the fuel cell [13].

As shown on Fig. 2 the system includes an interface cable through which the fuel cell is started up and shut down. Through this cable several system parameters are reported. A carbon-fiber cylindrical tank with an integrated 2-step pressure regulator and a gas-tube connector to connect the fuel cell to the tank are included too. The Aeropak system can alternatively be purchased with a hydride cartridge for easy of use [13].

The fuel cell weighs 470 g and measures 8 by 12 by 10.6 cm. The battery and power management card weight 208. The 1.1-litre tank shown on Fig. 2 weighs 1.12 kg, including the pressure reduction valve, has a diameter of 11 cm and a total length of 33 cm. A second 9-litre tank will be considered in the trade-off studies of section 3. This tank weights 5.62 kg and has a diameter of 18 cm for a total length of 64.4 cm.

2.2 Aerodynamics

2.2.1 Airfoil Selection

Several low Reynolds number airfoils were analyzed using XFOIL [14] for a wide range of Reynolds numbers. Fig. 3 shows the drag polars generated with XFOIL for the 3 airfoils that were down selected in the initial analysis. These 3 airfoils were chosen as they lead to the lowest drag at low Reynolds numbers. The full lines on the figure represent a Reynolds number of 200000 whereas the dashed lines are for 1000000.

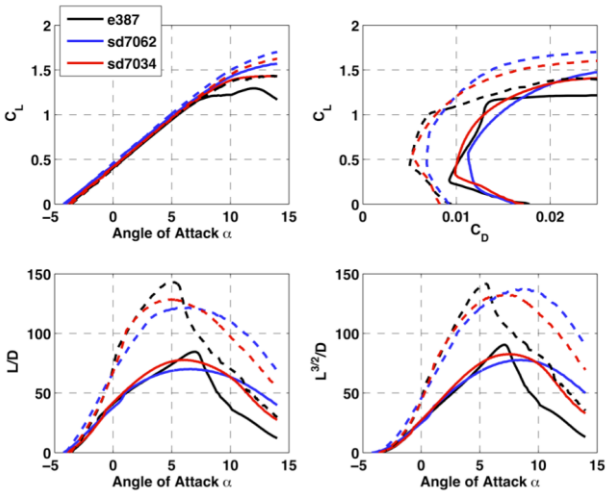

Fig. 3. Airfoil Drag Polars.

Out of the 3 airfoils, the sd7062 was retained as it has a significantly higher maximum lift coefficient than the other 2 candidate airfoils while maintaining a reasonable drag and pitching moment, especially at low Reynolds numbers [15]. The airfoil additionally has its maximum L/D and $L^{3/2}/D$ ratio at high lift coefficients, which is particularly important in low Reynolds number flight as the UAV will be flying close to its stalling angle [16].

2.2.2 Drag Estimation

The aircraft aerodynamic characteristics are determined using a mix of AVL [17] and

conventional textbook methods [18-20]. AVL is used to determine the zero-lift drag of the wing, using the airfoil polars generated through XFOIL. For the fuselage and the tailplane, the conventional flat plate analogy with form and interference factors is applied [18-20], as shown by the following equation for the fuselage (fus).

$$C_{D_0,fus} = \frac{\left(C_{f,lam}S_{wet,lam} + C_{f,turb}S_{wet,turb}\right)}{S_w}\left(1 + \frac{60}{(l/d)^3} + \frac{l/d}{400}\right)$$

where C_{D0} is the zero-lift drag coefficient, l and d the fuselage length and diameter, S_{wet} is the wetted area and S_w the wing area. C_f is the skin friction coefficient for the laminar (lam) and turbulent (turb) part of the fuselage. The laminar to turbulent transition is assumed to occur at the point of maximum thickness. A similar equation is used for the tail of the airplane [18-20]. The lift-induced drag is on the other hand calculated through AVL.

2.3 Component Weights and Centre of Gravity

2.3.1 Component Weight Correlations

To allow trade-off studies on various airframe parameters, component weight correlations from ref. [18-20] are used. As the correlations are intended for general aviation aircraft, they will give the right trends for UAV components but need to be "scaled" to UAV weights [21]. This is done using the "U" factors in the equations below [21]:

$$W_w = U_{ww} S_w^{0.694} AR_w^{0.5} (t/c)^{-0.4} (1+\lambda)^{0.1}$$

$$W_t = U_t S_t^{0.896} AR_t^{0.043} (t/c)^{-0.12}$$

$$W_{fus} = U_{fus} S_{wet}$$

$$W_{sys,av} = 0.052 W_{TO}^{0.843}$$

where S is the component area, S_{wet} its wetted area, AR stands for aspect ratio, λ for taper ratio and t/c is the thickness to chord ratio. The indices w, t, fus and sys,av represent wing, tail, fuselage and systems and avionics respectively. The "U" scaling factors used in this paper have been derived from the Georgia Tech fuel cell powered UAV as it is similar in size and extensive component weight data is available in the public domain [22]. Similar to the Georgia Tech design, the wing is tapered at the outer 30% of its span. A taper ratio of 0.67 is used and the tapered section uses a dihedral angle of 10 degrees to enhance lateral stability of the UAV.

As a wide range of wing aspect ratios is analysed in the trade-off studies described in section 3, a second wing weight correlation is added. As general aviation wings typically have a much lower aspect ratio, the validity of correlations based on these wings is namely questionable for some of the considered designs. A physical-based correlation is therefore used as no correlations were found for sailplane wing weights in the literature. The wing is assumed to be made of a foam core with 3 layers of fibreglass as skin. This structural arrangement is based on the SUAVE UAV previously built and flown at The University of Sydney [23,24]. The final wing weight is taken as the average of the two correlations.

The weight of the electronic speed controller and motor are based on commercial-of-the-shelf components. A 30% installation factor is adopted for all of the components placed inside the fuselage [21]. This installation factor covers the mountings of the components and any other additional weight required for their installation [21].

2.3.2 Centre of Gravity and Inertia

The centre of gravity (c.g.) of the aircraft is calculated for each phase of the mission to allow AVL to trim the UAV longitudinally with the elevator. The c.g. of the wing and tail are assumed to be at 42% of their respective mean aerodynamic chord [18, 19]. The c.g. of the fuselage is assumed to be at 48% of its length [18, 19]. The c.g. of the avionics and systems, payload and fuel are assumed to be in the centre of their respective "bays".

To estimate the static and dynamic stability of the aircraft, the moments of inertia around the 3 major axis of the UAV have to be known. The moments of inertia of the complete aircraft are estimated by AVL from the position of the individual components and their moments of inertia. To calculate the moments of inertia of the fuel cell, battery, brushless motors, avionics and payload, these components are considered

as solid cuboids. The moments of inertia of the wing, tails and fuselage are on the other hand based on their respective geometry and internal layout.

2.4 Flight Mechanics

2.4.1 Static and Dynamic Stability

The aircraft's static and dynamic stability are determined through AVL. An initial horizontal and vertical tail volume coefficient is set following guidelines from ref. [18-21]. As shown on Fig. 1, the wing position is subsequently changed to obtain a static margin of 15% of the wing mean aerodynamic chord. This was judged satisfactory for a fully autonomous UAV [21]. The vertical tail volume coefficient is on the other hand adapted to obtain a value of 0.04 for the $C_{n\beta}$ derivative. Whereas lower than suggested in [18], this value is in line with sailplane like designs of similar sizes [17] and leads to good stability characteristics for the UAV. All designs have a very lightly unstable phugoid and spiral mode but the modes have a high frequency and can thus easily be controlled. All other modes are stable. For the inverted V-tail designs reported in section 3, this $C_{n\beta}$ value furthermore leads to tail angles close to 50 degrees. This was judged desirable to ensure a high effectiveness of the control surfaces that act both as rudder and elevator.

2.4.2 Performance Estimation

The mission performance for the UAV is estimated using the so-called fuel fraction method [18-21]. The mission is split in several phases and for each phase the amount of fuel consumed is calculated using the Breguet range or endurance equation [18-21]. For each power setting, the fuel consumption used in the design calculations of this article is based on measured consumption from a hardware-in-the-loop (HWIL) test bench [25].

The fuel consumption was measured using this HWIL bench at several power settings; and the results are shown in Fig. 4. The black symbols in the figure indicate "stationary" points where the power level was maintained for a sufficiently long period to ensure that transient effects were negligible. The blue symbols on the other hand indicate "transient" point, where the power was maintained for only a relatively short period.

As shown in Fig. 4, the stationary fuel consumption was nearly linear up to 200 W, with a fuel consumption of approximately 2.25 sℓ/min at 200 W [25]. Above 200 W, the slope of the fuel-consumption curve changed as the battery began to contribute to the delivered power. At 300 W, the consumption was ~2.69 sℓ/min. At higher power settings, the fuel consumption leveled off at ~3 sℓ/min [25]. At that setting, the fuel cell supplied around 270 W; and the remainder of the demanded power came from the battery [25]. During transients, the fuel consumption varied significantly from the steady-state value.

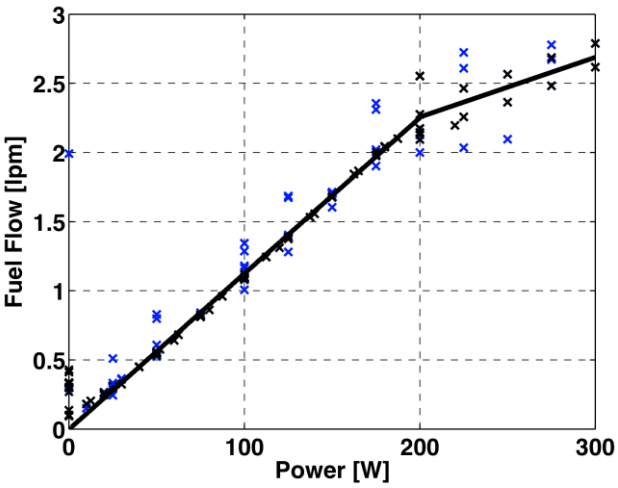

Fig. 4. Fuel-Cell Fuel Consumption [25].

3 Baseline Configurations and Tradeoff Studies

Four different wing parametric tradeoff studies were conducted to arrive at baseline designs. For each of the studies, the wing area and aspect ratio were varied to determine the optimum combination. The tradeoff studies were centered around 2 different tank sizes and 2 different configurations. Both the 1.1-litre and 9-litre carbon-fiber wrapped tanks mentioned in section 2.1 were used. For each of the tanks, both a pusher and a puller configuration were considered. For the puller configuration a single boom mounted T-tail was used, whereas the pusher aircraft were fitted with a twin boom mounted inverted V-tail. A single boom tail is

not feasible for the pusher configuration due to the propeller installation at the back of the fuselage. In the pusher configuration the payload is mounted in the front of the fuselage. With the puller configuration the payload is on the other hand positioned in the center of the fuselage.

The T-tail configuration was selected for ease of installation and to benefit from the winglet-effect of the horizontal tail on the vertical tail [18]. Both the horizontal and vertical tail have a taper ratio of 0.7. With the pusher configuration, the inverted V-tail was selected for its proverse roll-yaw coupling [18]. Below the 4 different studies are reported. The design mission and payload data are detailed first. After that, the 9-litre tank designs are reported. Section 3.3 finally gives the results of the parametric study for the 1.1-litre tanks.

3.1 Design Mission and Payload

The main advantage of the fuel cell over conventional electrical propulsion lies in the increased endurance capability of the platform. As such the primary mission was set up as a typical over-the-hill surveillance mission. The mission profile that was adopted for this mission is shown in Fig. 5. As the figure shows the UAV initially climbs to its cruising altitude of 500 ft. During climb the maximum power of the hybrid system is used (600 W) and the UAV is assumed to fly at 35 kts. Once the UAV reaches an altitude of 500 ft, it cruises to its loitering zone. That zone is assumed to be 10 nm from the point where the cruise altitude is reached. The UAV cruises at 40 kts. Once its destination is reached the UAV enters a loiter pattern with a 15 degree bank angle. The loiter speed is assumed to be 35 kts. The UAV loiters until just enough fuel is left to return to its base. Before landing a 5 min loiter phase is added to account for possible airport traffic.

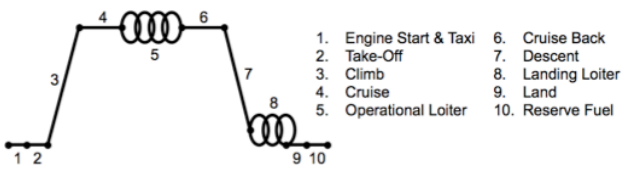

Fig. 5. Mission Profile.

For all of the parametric studies the UAV is equipped with a 2.5 kg payload that consumes 50 W. This payload capability allows fitting a variety of equipment for typical surveillance or observation missions. The payload could consist of a nano SAR [26], a multi-spectral electro-optical and infrared camera [27-28] or a variety of meteorological sensors [29]. The payload is assumed to consume power only during the loiter phase. For the remainder of the mission, the payload is switched off and does not consume any power.

3.2 9-litre Tank

Fig. 6 shows the results of the parametric study for the puller T-tail configuration using the 9 litre tank. The black lines in the figure indicate the power required during cruise, the red lines give the power required during the loiter phase. The blue lines give takeoff weight, whereas endurance is depicted in purple. Several zones of the figure are shaded, showing restrictions on the design space. The yellow zones indicate design solutions where the Reynolds number of the wing (straight line going to the upper right) and the horizontal tail fall below the cutoff Reynolds number of 200,000. This limit is imposed to avoid laminar separation bubbles as they lead to an unstable pitch behavior and a sharp drag increase [16]. The green zone marks a stall margin of 1.15 for the loiter phase [21]. This margin is added to avoid stall when hit by a gust. A similar margin was added for cruise but this did not affect the design space as cruise is flown at a lower lift coefficient. The black zone indicates designs where the cruise power is higher than the nominal fuel-cell power of 200 W. The zone shaded in red indicates a similar power limit for the loiter phase.

As shown on Fig 6 the design point was selected at a wing area of 1.27 m^2 whereas the design aspect ratio is 28.7. With this combination a loiter endurance of 24.4 hours is achievable with a takeoff weight of 18.2 kg. In loiter, the fuel cell needs to provide 178 W to the motor and payload whereas 158 W is required in cruise.

Fig. 7 gives the weight breakdown for the selected design point. As shown, the installed

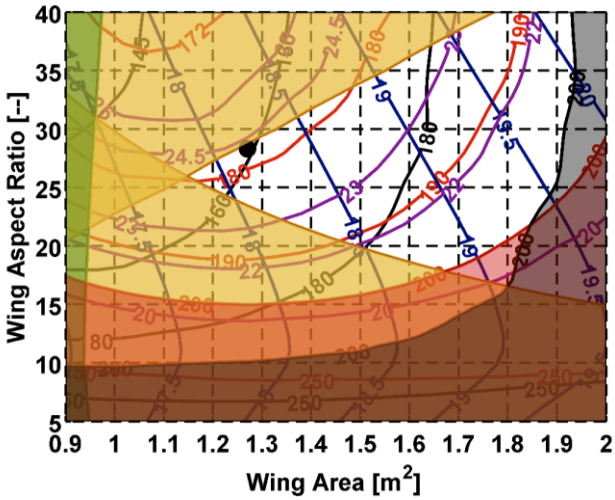

Fig. 6. Parametric study for the 9 litre T-tail.

payload represents 18% of the takeoff weight of the aircraft. Installation of the components inside the fuselage represents another 12% of the takeoff weight. Due to the high lower heating value of hydrogen and its low density, fuel represents only 1% of the takeoff weight. The fuel cell, motor and ESC account for only 7% of the takeoff weight. The tank is by far the heaviest component and makes up 33% of the takeoff weight.

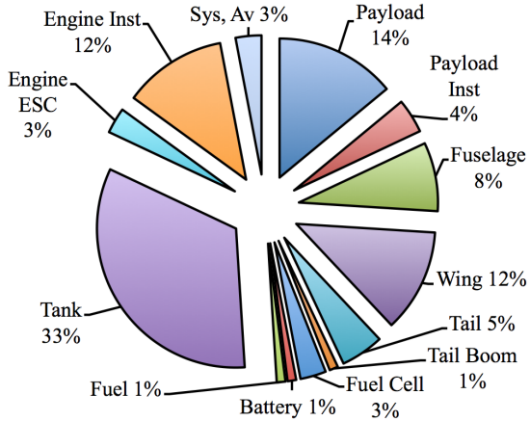

Fig. 7. Weight Breakdown for the 9-litre V-tail design.

Fig. 8 shows the results of a similar tradeoff study for the inverted V-tail pusher configuration for the same design mission and tank configuration. As the figure shows, the horizontal tail Reynolds number limit affects a much smaller zone of the design space. As the horizontal and vertical tail sizes are coupled and the vertical tail is sized to provide a $C_{n\beta}$ derivative of 0.04, a slightly higher horizontal tail chord is obtained than in the T-tail case. The figure also shows that this configuration leads to a slight increase in loiter endurance (24.9 hrs instead of 24.4 hrs) but the takeoff weight increases to 18.5 kg. The wing that leads to the maximum loiter endurance is slightly bigger (1.30 m^2) and has a slightly higher aspect ratio (29.0).

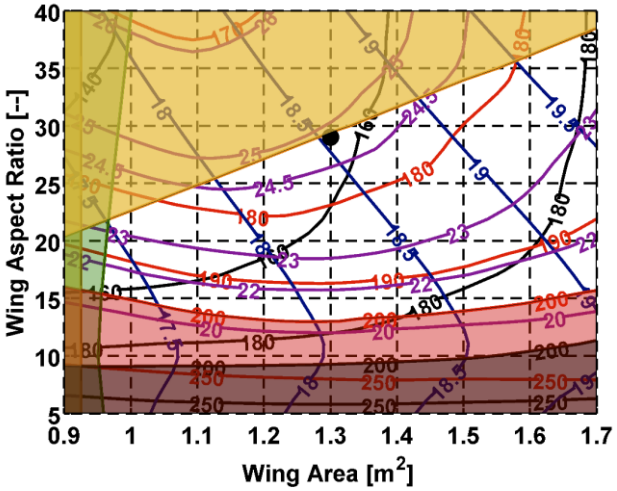

Fig. 8. Parametric study for the 9 litre V-tail.

Table 1 summarizes the major features of both configurations using the 9-litre tank. As shown in the table the increase in endurance predominantly comes from the slightly lower power required in cruise. The reduced drag of the higher aspect ratio wing more than offsets it increase in weight, resulting in a design that has a slightly higher endurance, but also a slightly higher takeoff weight.

Table 1. Comparison between both 9-litre configurations.

	T-tail	V-tail
Wing Area [m^2]	1.27	1.30
Wing Aspect Ratio [--]	28.7	29.0
Wing Span [m]	6.04	6.14
Takeoff Weight [kg]	18.2	18.5
Cruise Power [W]	158	157
Loiter Power [W]	178	175
Endurance [hrs]	24.4	25.0

3.3 1.1-litre Tank

Fig. 9 gives the results for the parametric study of the T-tail puller configuration with a 1.1-litre tank. As in the design studies for the 9-litre tank, the Reynolds number of the horizontal tail of the T-tail imposes a big restriction on the

feasible design space. For the smaller tank, none of the other restrictions play a role in the investigated design space. Due to its smaller size, the UAV loiters at just under 140 W of fuel cell power and during cruise only 121 W is needed. A wing area of 1.12 m^2 and an aspect ratio of 25.2 lead to the maximum loiter endurance. With this wing, a loiter endurance of 3.7 hours is possible. As shown on Fig. 9 the UAV is significantly smaller than the 9-litre tank designs and weighs in at 10.5 kg.

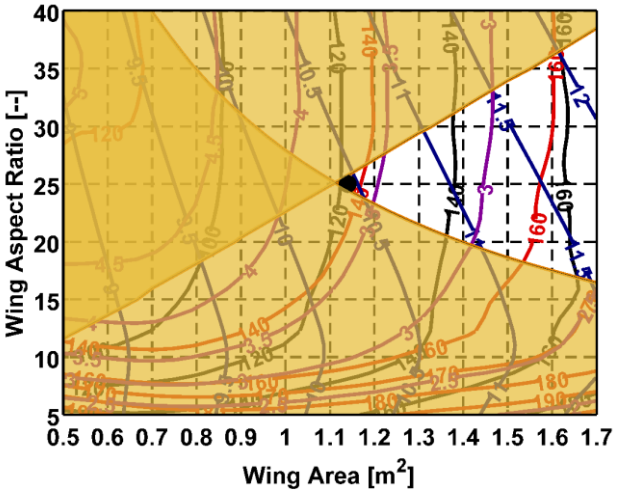

Fig. 9. Parametric study for the 1.1 litre T-tail.

Fig. 10 gives a very similar picture for the V-tail puller configuration. Again only the Reynolds number limits are of importance. Due to the slightly smaller horizontal tail a reduction in wing area (from 1.12 m^2 to 0.93 m^2) is possible, which leads to a much lower wing aspect ratio of 20.8. As a consequence the UAV takeoff weight is reduced to 9.9 kg and the loiter endurance increases to 4.9 hrs.

Fig. 11 gives the weight breakdown for the 1.1-litre V-tail UAV. As shown in the figure, the installed payload now represents 31% of the takeoff weight, compared to 24% for the 9-litre design. Fuel only represents 0.2% of the weight compared to 1% for the 9-litre design. The most significant change is related to the tank weight, which has gone down from 33% for the 9-litre UAV to 11% for the 1.1-litre design. The structural weight has on the other hand grown in relative importance. The wing and tail now represent 27% of the takeoff weight compared to 18% for the 9-litre design.

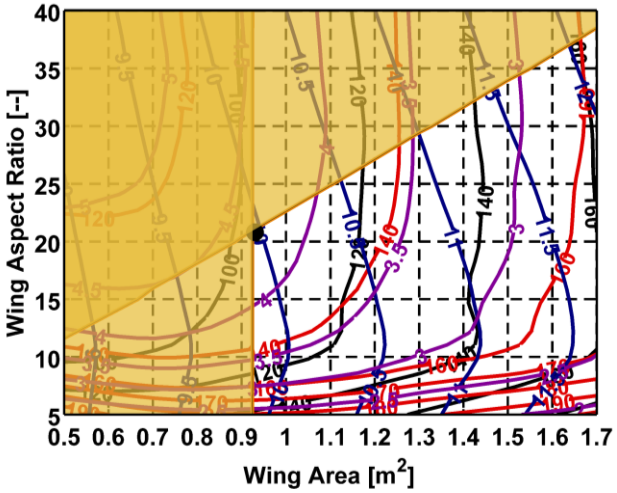

Fig. 10. Parametric study for the 1.1 litre V-tail.

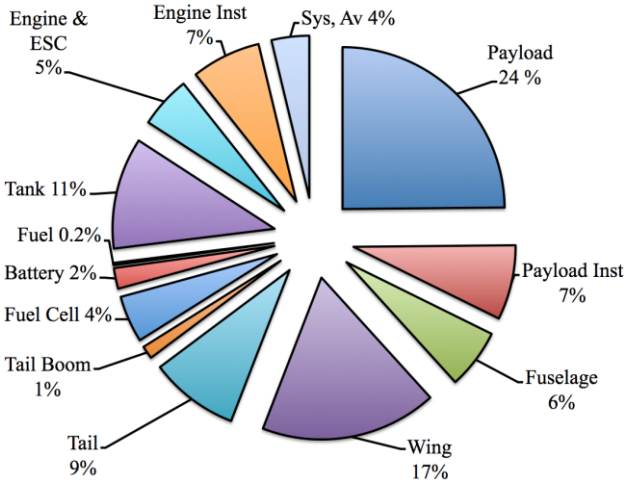

Fig. 11. Weight Breakdown for the 1.1-litre V-tail design.

Table 2 summarizes the comparison between the two configurations for the 1.1-litre tank. The table shows that the significant reduction in wing area and aspect ratio results in a considerably lighter overall design. As a consequence the power required in loiter is 10 W lower for the V-tail design than for the T-tail configuration. This leads to an increase in endurance of about 16%.

Table 2. Comparison between both 1.1-litre configurations.

	T-tail	V-tail
Wing Area [m^2]	1.12	0.93
Wing Aspect Ratio [--]	25.2	20.8
Wing Span [m]	5.31	4.40
Takeoff Weight [kg]	10.5	9.9
Cruise Power [W]	121	103
Loiter Power [W]	138	128
Endurance [hrs]	3.7	4.3

4 Fuel Cell Installation in the demonstrator

In order to limit the cost associated with the manufacturing of the demonstrator UAV, it was decided to use a previously designed UAV as the demonstrator platform. The demonstrator will thus be based on the SUAVE (Small UAV for Experimentation) platform of the School of Aerospace, Mechanical and Mechatronic Engineering of The University of Sydney [22,23]. The SUAVE is a small and flexible platform with a takeoff weight around 8 kg, and an empty weight of 4.2 kg in its original design of 2004-2005. The SUAVE has been designed in 2 different configurations: one with a T-tail and one with a single boom V-tail. Both designs had a common wing with a wing area of 0.85 m^2 and an aspect ratio of 9 [22,23]. As the platform was designed for experimentation, the tail surfaces are comparatively big and a static margin of 30% was adopted [22,23]. Fig. 12 shows the SUAVE UAV on its catapult launcher.

Fig. 11. The SUAVE UAV on its launcher.

Both SUAVE configurations are pullers and use a common fuselage. The fuselage was designed for flexibility seen the original intend of the design: a UAV for experimentation. As such the fuselage has a diameter of 22 cm, which is more than sufficient to install the 1.1-litre tank and the fuel-cell based hybrid system. For ease of installation and access in between test flights, it was decided to install the components of the fuel-cell based system on a tray that can slide in and out of the fuselage by removing the nose cap. Fig. 13 shows the design of the tray.

The figure shows how all the components are fitted on a fiberglass-reinforced balsa wood tray. The tank is strapped to 2 support systems. The fuel cell (black) on the other hand is held in place by 2 rails. As shown, the SUAVE is reconfigured as a pusher airplane

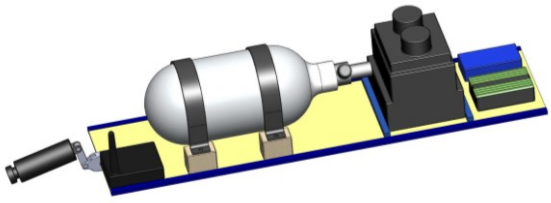

Fig. 13. Installation tray for the fuel-cell system.

to allow a front camera as payload for the demonstration flights. Fig. 14 shows the tray installed in the SUAVE UAV. As shown in the figure, the original fuselage of the SUAVE provides ample room for the installation of the entire system. The figure also shows how the tray is supported inside the fuselage on 4 different brackets that are built into the belly of the fuselage.

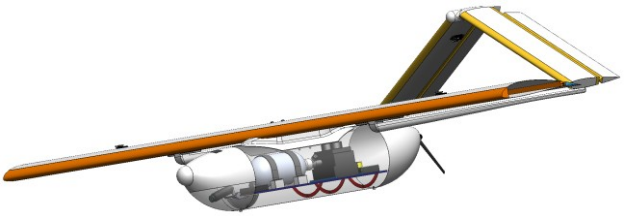

Fig. 14. Fuel cell system installed in the reconfigured SUAVE.

5 Conclusions

This paper presents the preliminary design of a fuel-cell based hybrid-electrical UAV. Wing design parametric studies are presented for 2 different configurations and 2 different tank sizes. For both tank sizes, the inverted V-tail designs have a slightly higher endurance. For all of the considered configurations, the wing design space is severely limited by the need to avoid laminar separation bubbles. Horizontal tail Reynolds numbers only impose a restriction for the smaller tank designs. With the higher tank size the optimum endurance can be reached without being restricted by laminar separation bubbles on the horizontal tail.

The parametric studies show that an endurance in loiter of 4.3 hours is feasible with a 1.1-litre tank. With this tank the UAV has a take-off weight of around 10 kg. With a 9-litre tank an endurance of 25 hours can be attained for a takeoff weight of 18.5 kg.

The final section of the paper showed the installation of the fuel-cell based hybrid system on an existing platform. That platform

will be used as a demonstrator in the future phase of the program.

References

[1] Shin Y, Chang S-H, et al. Performance test and simulation of a reciprocating engine for long endurance miniature unmanned aerial vehicles, *Proc Inst Mech Eng, Pt D: J Auto Eng*, Vol. 219, No. 4, pp. 573–581, 2005.

[2] Thomas JP, Qidwai MA, et al. Energy scavenging for small-scale unmanned systems, *J Pwr Src*, Vol. 159, No. 2, pp. 1494–1509, 2006.

[3] Kim K, Kim T, et al. Fuel cell system with sodium borohydride as hydrogen source for unmanned aerial vehicles, *J Pwr Src*, Vol. 196, pp. 9069–9075, 2011.

[4] Rhoads GD, Wagner NA, et al. Design and flight test results for a 24 hour fuel cell unmanned aerial vehicle, *8th Ann Intl Ener Conv Eng Conf*, Nashville, AIAA-2010-6690, 2010.

[5] De Garmo MT. Issues Concerning Integration of Unmanned Aerial Vehicles in Civil Airspace, *MITRE*, MP 04W0000323, Nov 2004

[6] Honeycutt, G. Next-Generation Power – Fuel Cells Set Records, Turn Head, *Unmanned Systems*, May 2010.

[7] Bradley TH, Moffitt BA, et al. Development and experimental characterization of a fuel cell powered aircraft. *J Pwr Src*, Vol. 171, No. 2, pp. 793–801, 2007.

[8] Verstraete D, Steimes J, et al. Conceptual design of a PEM fuel cell powered unmanned aerial vehicle, *Proc 8th Ntl Cong Theo App Mech*, Brussels, Belgium, 2009.

[9] Hendrick P, Verstraete D, et al. Preliminary Design of a mini-UAV using a Fuel Cell Propulsion System, *Proc NATO RTO AVT Symp Novel Vehicle Concepts and Emerging Vehicle Techn*, RTO-MP-104, Brussels, April 2003.

[10] Kim M-J and Peng H. Power management and design optimization of fuel cell/battery hybrid vehicle, *J Pwr Src*, Vol. 165, No. 2, pp. 819–832, 2007.

[11] Burke AF. Batteries and ultracapacitors for electric, hybrid, and fuel cell vehicles, *Proc IEEE: Elec Hyb Fuel Cell Veh*, Vol. 95, No. 4, pp. 806–820, 2007.

[12] Romeo G, Borello F, et al. Set –Up and Test Flights of an All-Electric Aeroplane Powered by Fuel Cells, *J Acft*, Vol. 48, No. 4, pp. 1331–1341, 2011.

[13] Horizon Energy Systems, Pte. Ltd. *Aeropak Technical Data Sheet*. 2010. Available at: http://www.hes.sg/files/AEROPAK_Technical_Data_Sheet.pdf.

[14] Drela M. XFOIL source code, manual and examples, *http://web.mit.edu.drela/Public/web/xfoil/*, accessed: December 2011.

[15] Coiro DP, Nicolosi F. Design of a Three Surfaces R/C Aircraft Model, *Acta Polytechnica*, Vol. 42, No. 1, pp. 4-53, 2002.

[16] Mueller TJ, Torres GE et al. Elements of Aerodynamics, Propulsion and Design, *Introduction to the Design of Fixed-Wing Micro Air Vehicles*, Chapter 2, AIAA Education Series, Reston, VA, 2007.

[17] Drela M. AVL source code, manual and examples, *http://web.mit.edu.drela/Public/web/avl/*, accessed: December 2011.

[18] Raymer D. *Aircraft Design: A Conceptual Approach*, 3rd edition, AIAA Education Series, Reston, VA, 1999.

[19] Roskam J. *Airplane Design, Parts I-VIII*, Darcorporation, Kansas, KA, 1997.

[20] Nicolai L, Carichner G. *Fundamentals of Aircraft and Airship Design*, Vol 1, AIAA Education Series, Reston, VA, 2010.

[21] Chaput A. *Conceptual Design of UAV Systems,* Short Course Lecture Notes, Kansas University Continuing Education, Bethesda, MD, 2007.

[22] Bradley TH, Moffitt BA, et al. Development and experimental characterization of a fuel cell powered aircraft. *J Pwr Src*, Vol. 171, No. 2, pp. 793–801, 2007.

[23] Srilertchaipans T. *Small Unmanned Aerial Vehicle for Experimentation (SUAVE): Design using Multidisciplinary Optimization*, Honours Thesis, The University of Sydney, 2005.

[24] Webb JC, *The Small Unmanned Aerial Vehicle for Experimentation: The Design and Manufacture of the Fuselage, and Powerplant Selection,* Honours Thesis, The University of Sydney, 2004.

[25] Verstraete D, Harvey J, and Palmer J. Hardware-in-the-loop simulation of fuel-cell-based hybrid-electrical UAV propulsion, *Proc 28th Int Cong of the Aero Sci*, Brisbane, Australia, 2012.

[26] imSAR, *NanoSAR – Denying the Enemy Sanctuary*, imSAR brochure, 2008

[27] Berni JAJ, Zarco-Tejada PJ, Suarez L, Gonzalez-Dugo V, Fereres E, Remote Sensing of Vegetation from UAV Platforms Using Lightweight Multispectral and Thermal Imaging Sensors, *Proc ISPRS Hannover Workshop*, Hannover, Germany, 2009.

[28] Nebiker S, Annen A, Scheere M and Oesch D, A Light-Weight Multispectral Sensor for Micro UAV – Opportunities for Very High Resolution Airborne Remote Sensing, *Proc ISPRS Beijing Workshop,* Vol. XXXVII, Part B1, Beijing, China 2008.

[29] Patterson MCL, Brescia A, Operation of Small Sensor Payloads on Tactical Sized Unmanned Air Vehicles, *The Aeronautical Journal*, Vol. 114, No. 1157, pp, 427-436, 2010.

Copyright Statement